

Supplement of Atmos. Chem. Phys., 19, 14703–14720, 2019  
<https://doi.org/10.5194/acp-19-14703-2019-supplement>  
© Author(s) 2019. This work is distributed under  
the Creative Commons Attribution 4.0 License.



*Supplement of*

## **Predominance of secondary organic aerosol to particle-bound reactive oxygen species activity in fine ambient aerosol**

**Jun Zhou et al.**

*Correspondence to:* Josef Dommen ([josef.dommen@psi.ch](mailto:josef.dommen@psi.ch)) and Ru-Jin Huang ([rujin.huang@ieecas.cn](mailto:rujin.huang@ieecas.cn))

The copyright of individual parts of the supplement might differ from the CC BY 4.0 License.

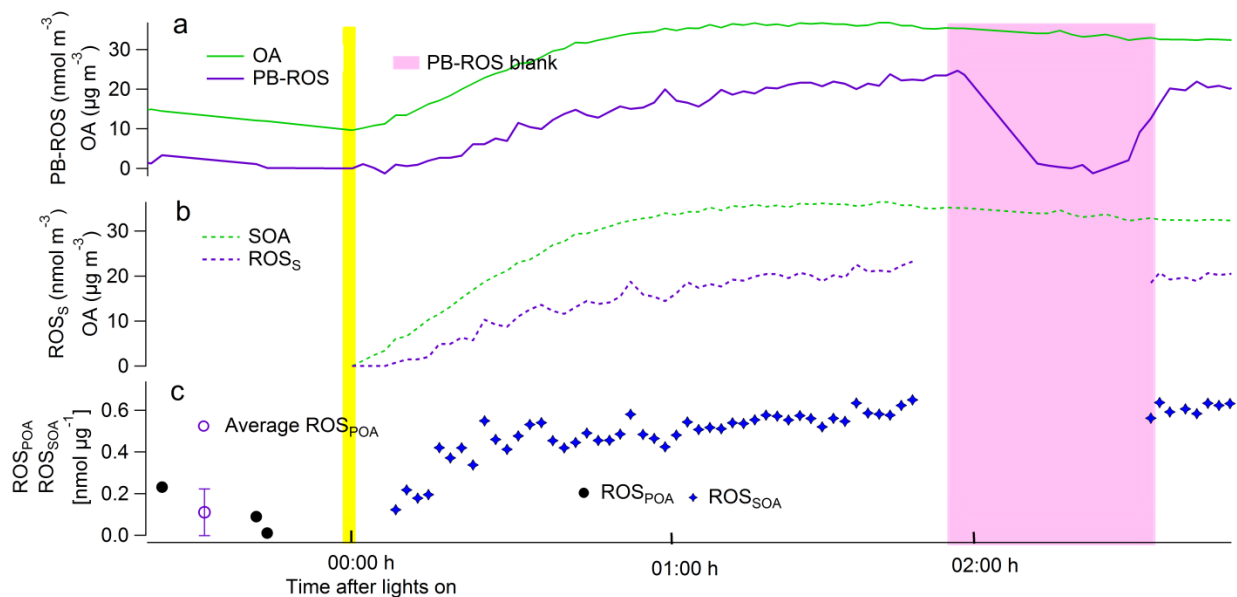


**Figure S1:** Evolution of the ROS content in SOA during a coal burning smog chamber aging experiment. (a) Total OA and ROS, (b) SOA and ROS<sub>S</sub>, (c) ROS content in POA (ROS<sub>POA</sub>, before lights on) and ROS<sub>S</sub> content in SOA (ROS<sub>SOA</sub>, after lights on). The pink area represents the ROS blank measurement.

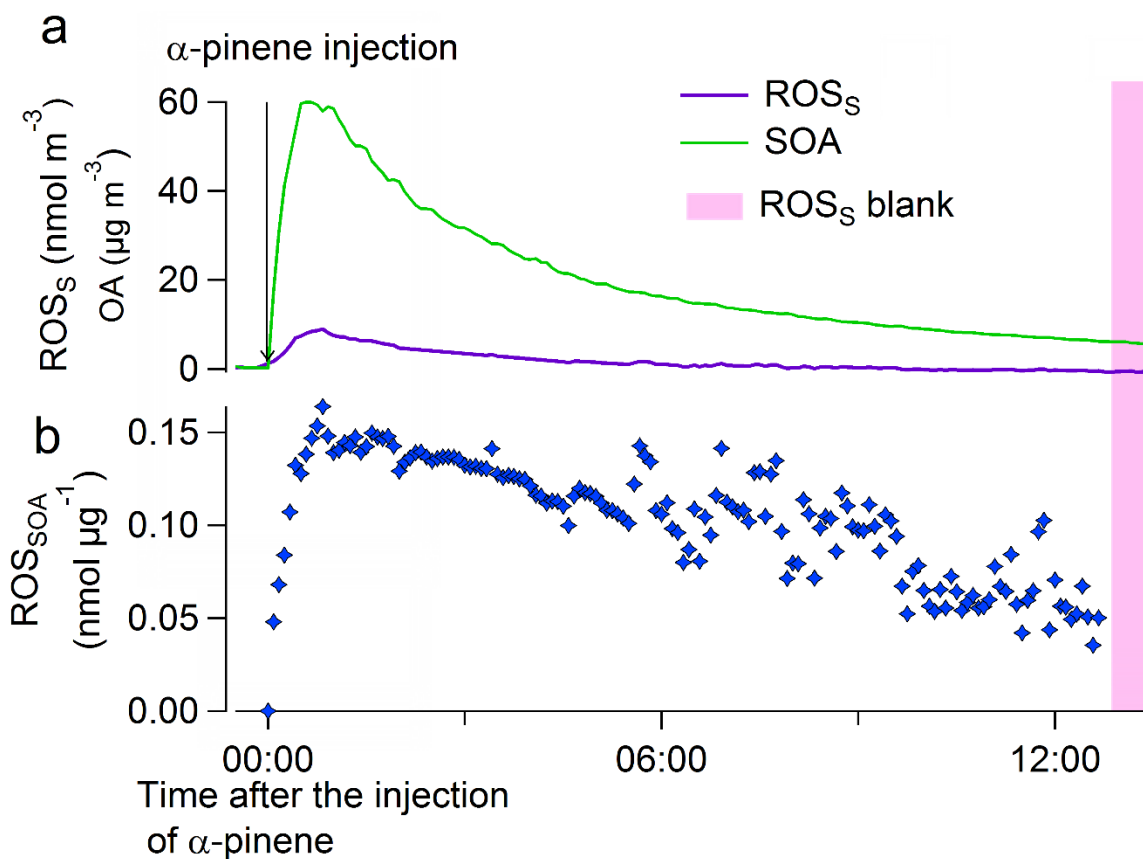


**Figure S2:** Evolution of (a) SOA and ROS<sub>S</sub>, and (b) ROS<sub>S</sub> content in the SOA (ROS<sub>SOA</sub> = ROS<sub>S</sub>/SOA) concentrations measured during an α-pinene ozonolysis experiment in the smog chamber. The pink area represents the ROS blank measurement.

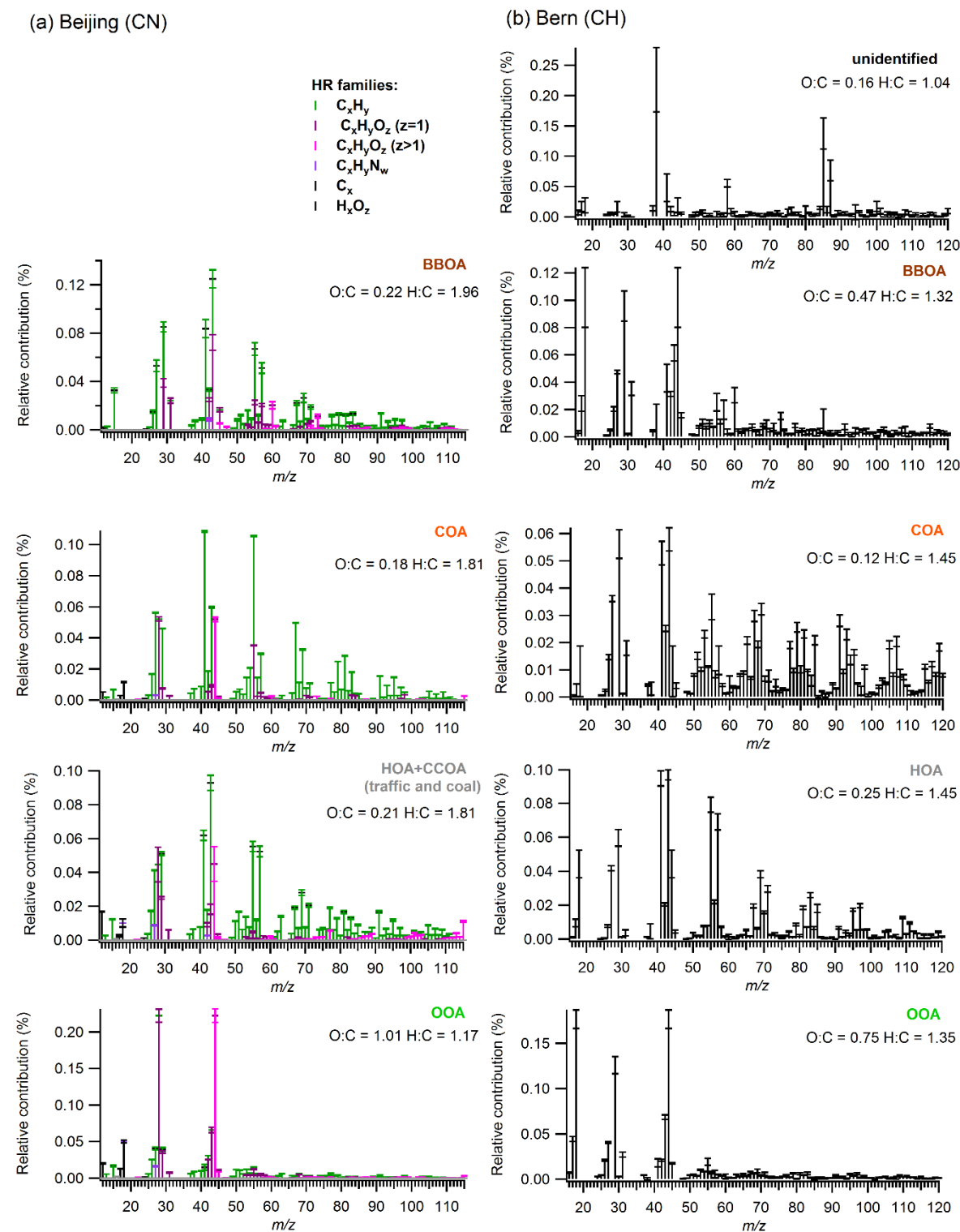
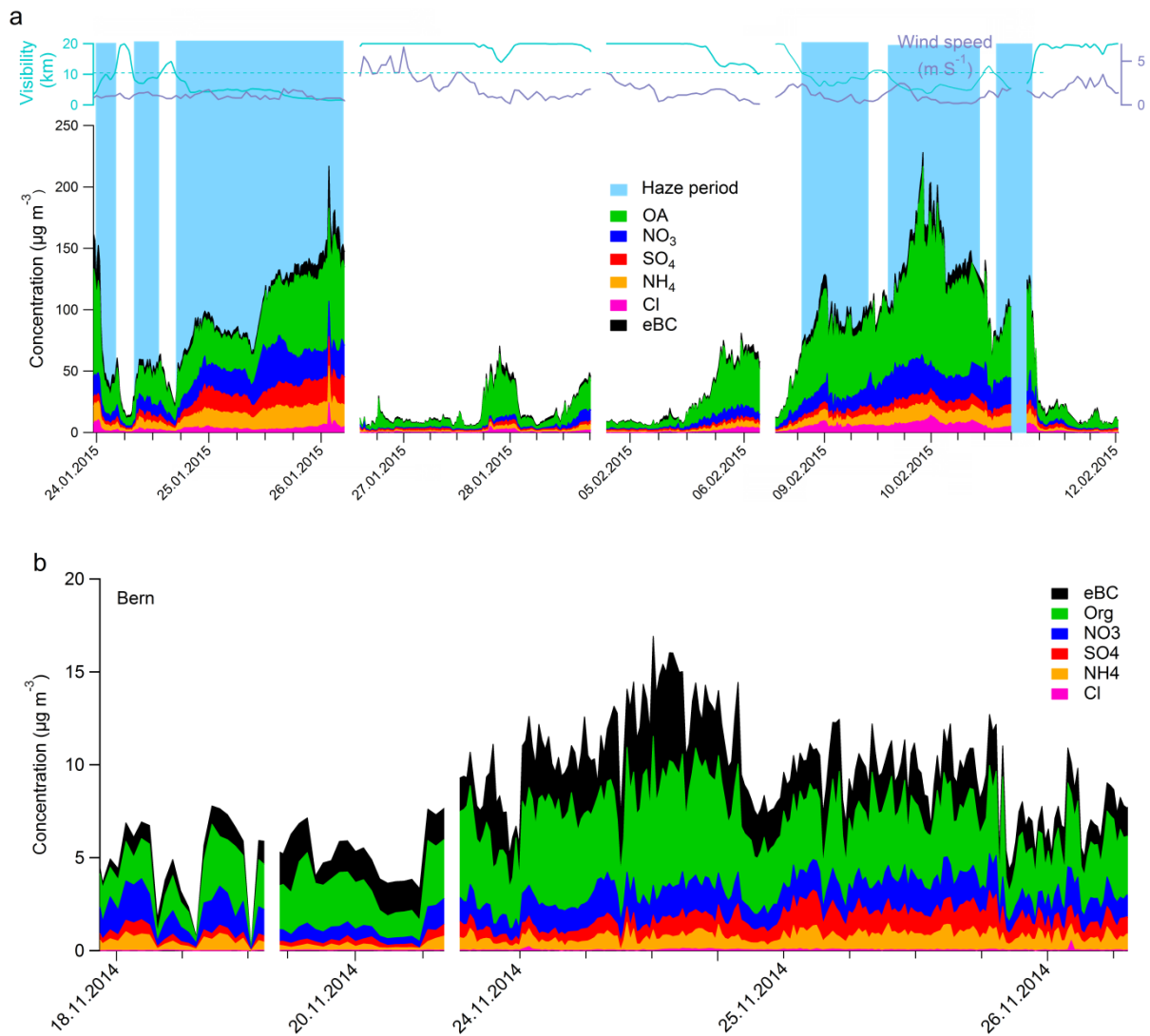


**Figure S3:** Mass spectra of the identified OA factors for (a) Beijing and (b) Bern, color-coded with the chemical families. Spectra are averaged over all good a-value combinations (see Section 2.3). Error bars represent one standard deviation of each  $m/z$  over all the accepted solutions. In Bern, the mass spectra were obtained from the unit mass resolution-ACSM. O:C was calculated according to Aiken et al. (2008), and H:C was estimated according to Ng et al. (2011).

5

5 Figure S4a and Fig. S4b show temporal variations of the non-refractory chemical components (including organic aerosol (OA),  $\text{SO}_4$ ,  $\text{NO}_3$ ,  $\text{NH}_4$ , Cl) concentrations and equivalent black carbon (eBC) measured by either an AMS or an ACSM, and an aethalometer during the measurement periods January-February 2015 in Beijing and November 2014 in Bern. In Beijing, the periods highlighted with a blue background represent the haze periods, which were defined by a visibility of less than 10 km. The remaining periods are classified as reference periods (with a visibility above 10 km).



10 **Figure S4:** Time series of non-refractory chemical components and eBC in (a) Beijing and (b) Bern during the measurement periods.

15

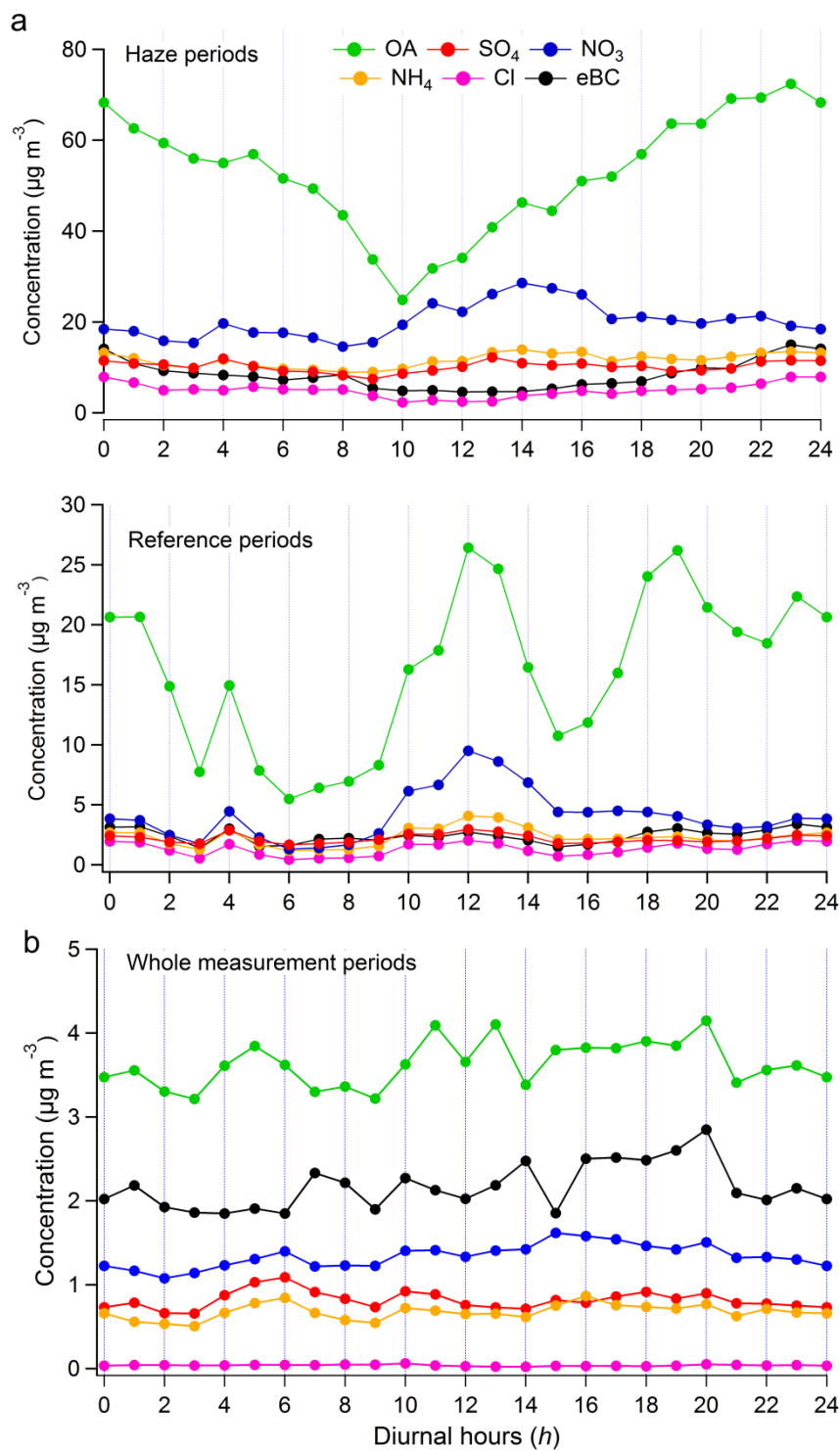
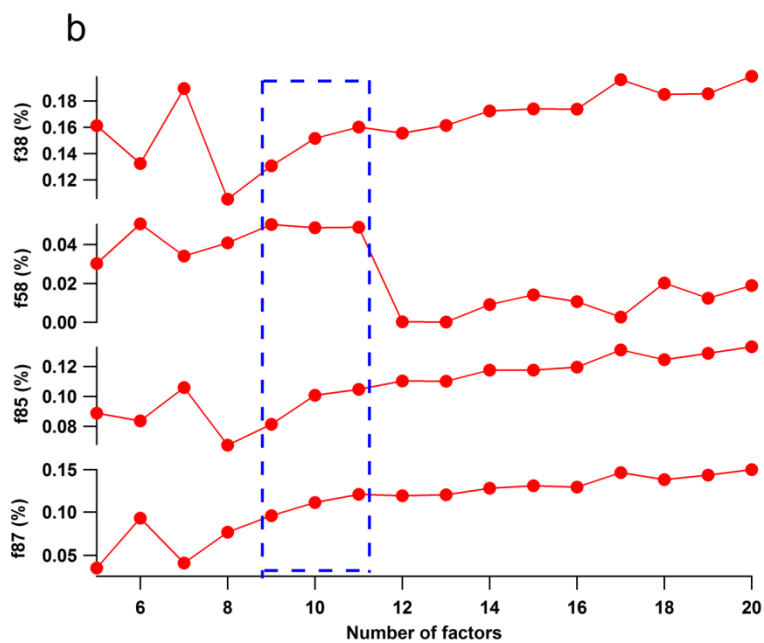
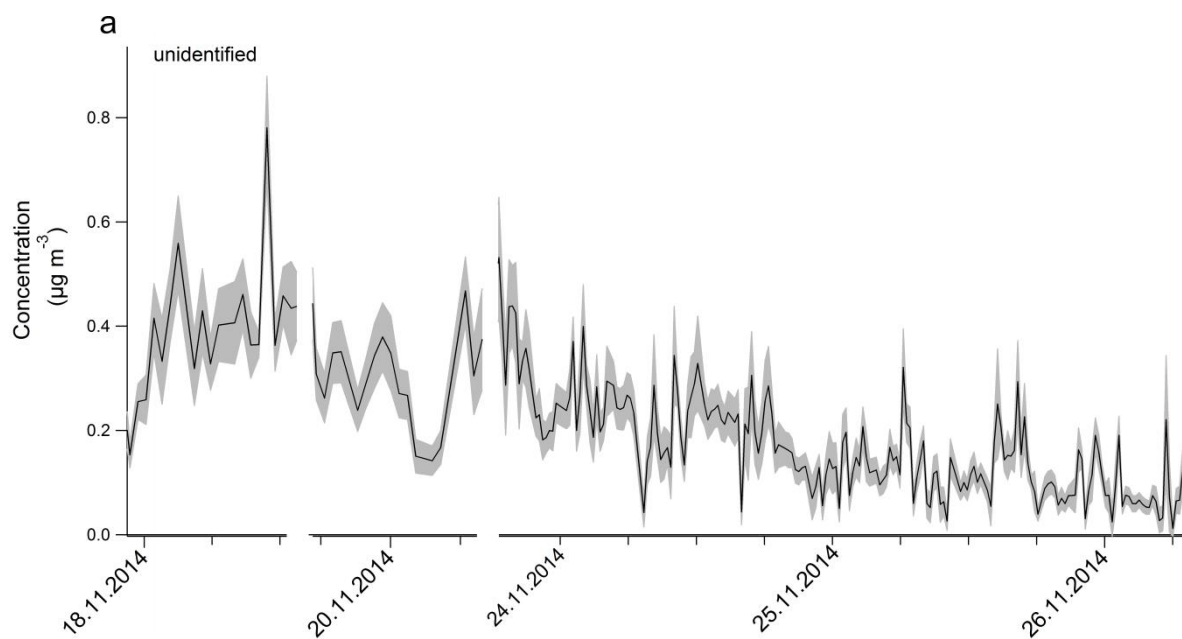
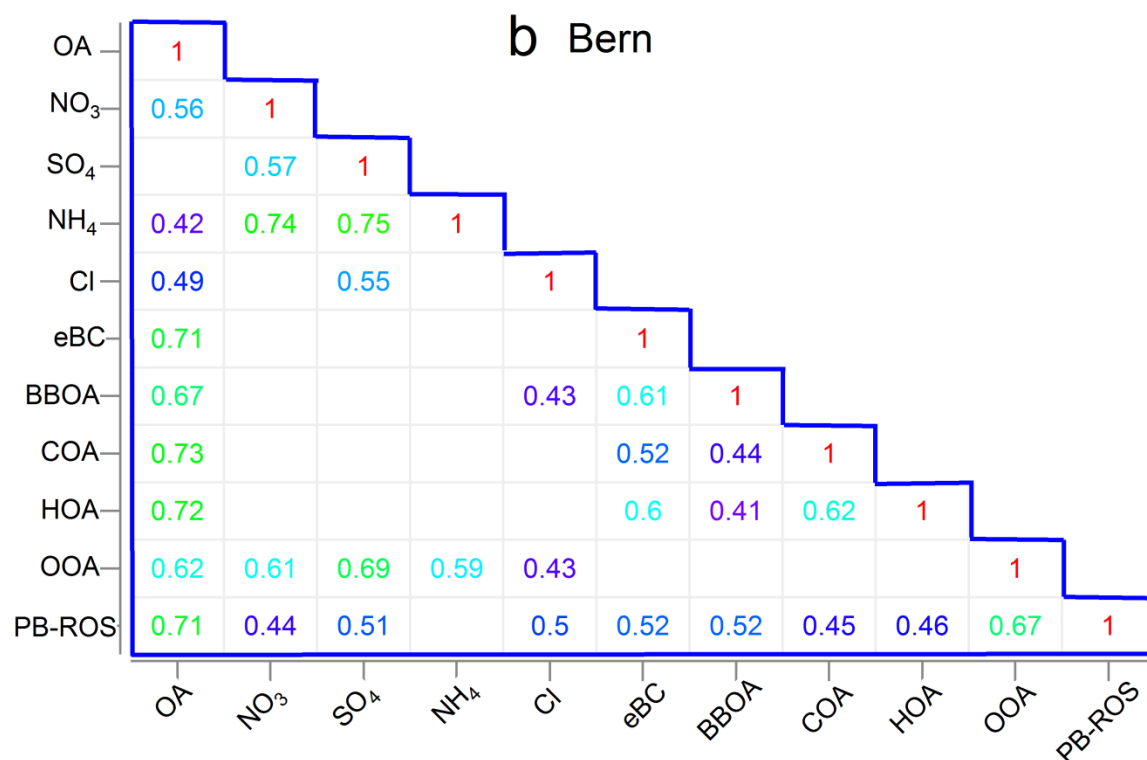
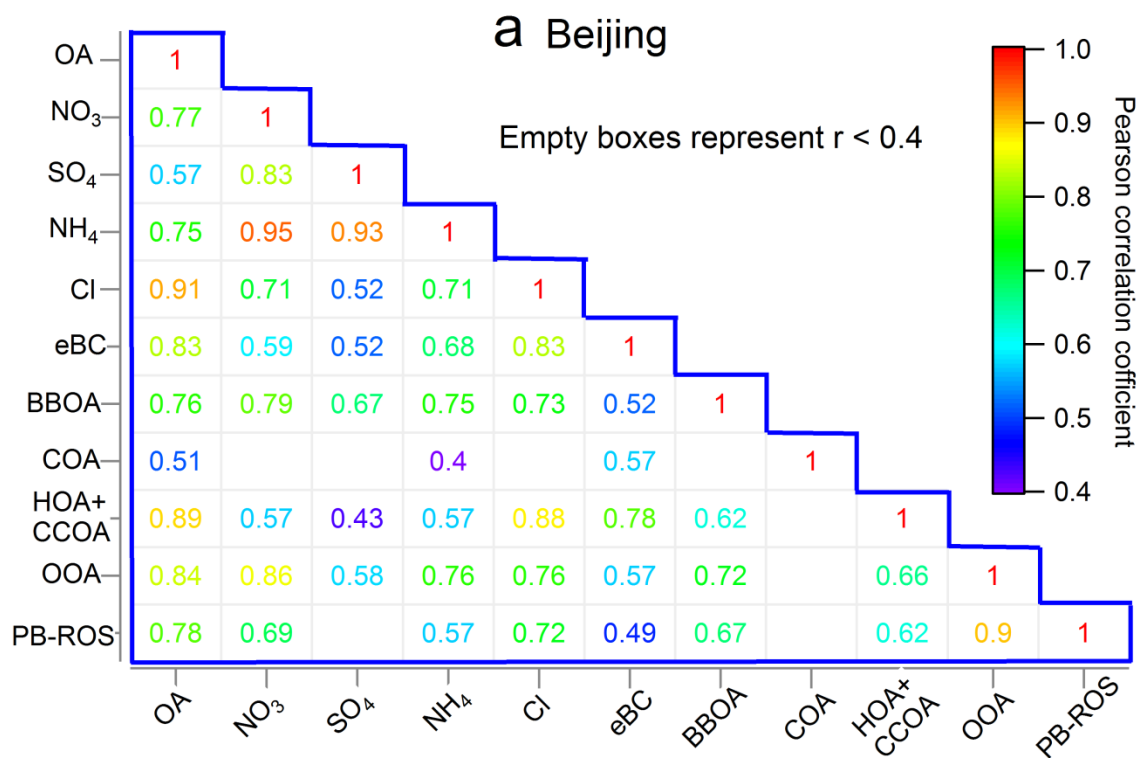


**Figure S5:** Average diurnal trends of mass concentrations of all chemical components measured during the campaigns in (a) Beijing and (b) Bern.



(b)

**Figure S6:** Evaluation of the unidentified factor. (a) time series of the unidentified factor in Bern and (b) changes in the most important  $m/z$ -fractions of this factor for an increasing number of factors. The unidentified mass spectra obtained from the 9-, 10-, and 11-factor solutions labeled in the blue rectangle were used in the source apportionment analysis.



5 **Figure S7:** Correlation matrix showing Pearson's  $r$  for the chemical composition and OA components in (a) Beijing and (b) Bern during the corresponding measurement periods.

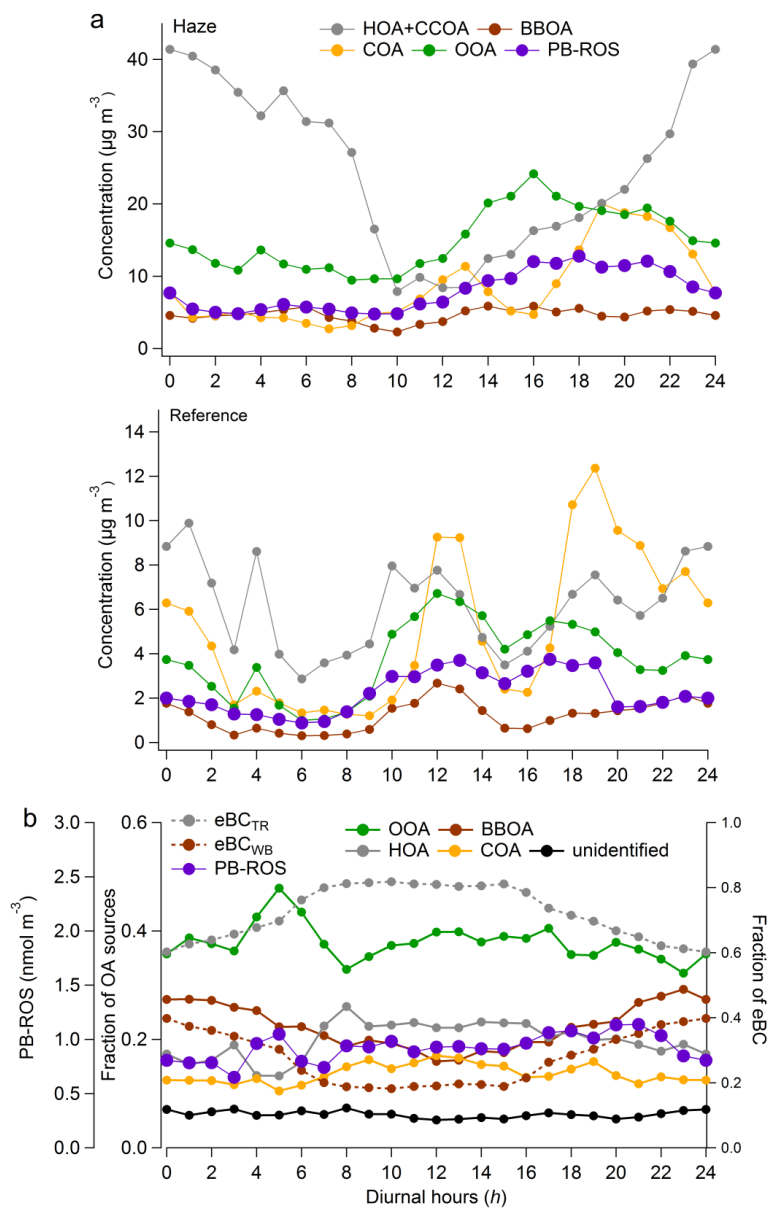


**Figure S8:** Average diurnal patterns of the concentrations of OA components during the measurement periods in (a) Beijing and (b) Bern. In Bern, the diurnal variations of PB-ROS as well as the PMF factors OOA, BBOA, HOA, COA, and unidentified are shown as fraction of OA sources, and the eBC fractions from traffic (eBC<sub>TR</sub>) and wood combustion (eBC<sub>WB</sub>) are shown as fraction of eBC.

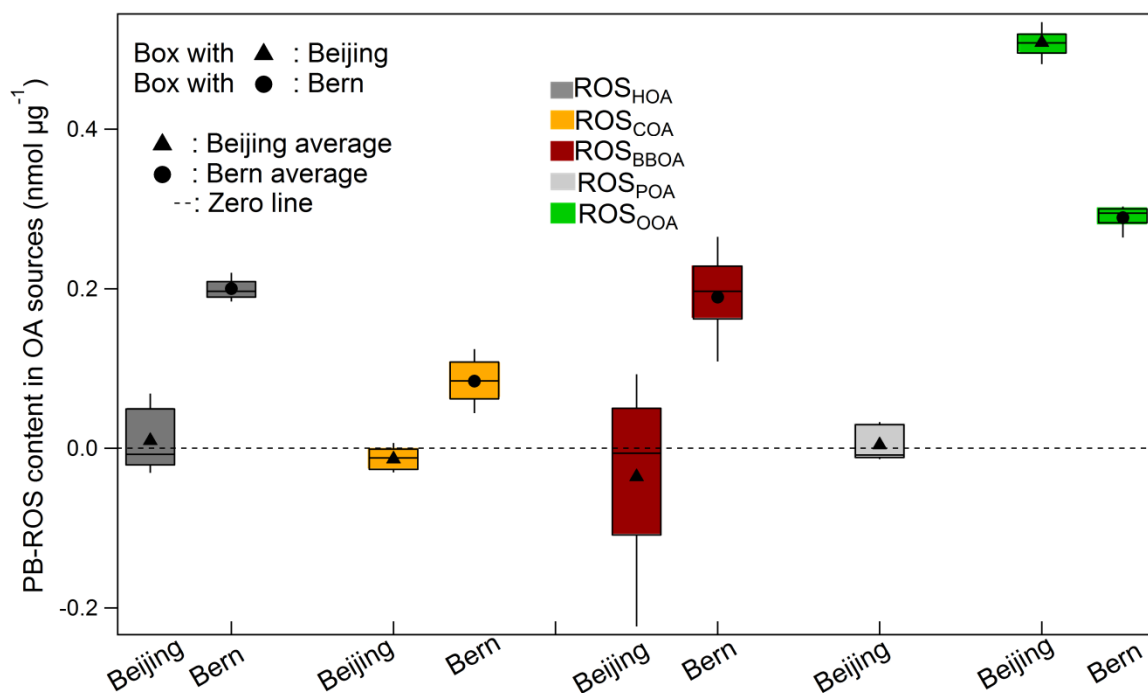


**Figure S9:** Box plots of the regression coefficients of ROS with different OA sources obtained from the multiple linear regression model (MLRM) of the ambient data of Beijing (triangle) and Bern (solid circle). The bottom and the top of the box are the first and third quartiles. The horizontal line inside the box is the median of the data. The vertical line through the box connects the data from minimum to maximum.

5

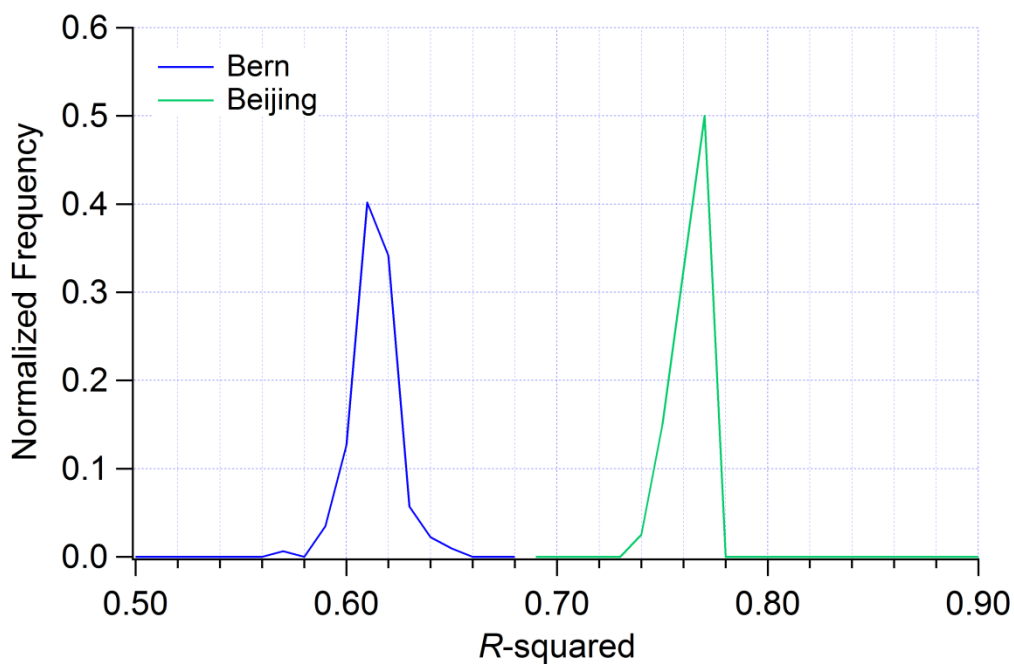
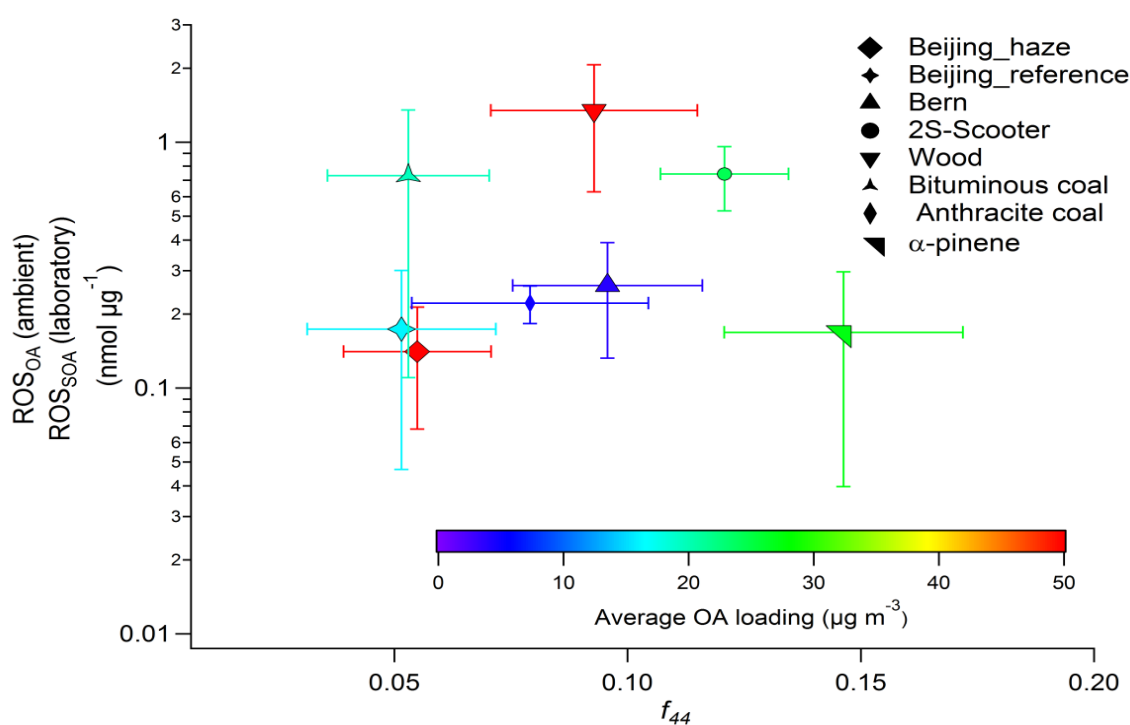


**Figure S10:** Normalized frequency distributions of adjusted  $R$ -squared obtained from the MLRM in Beijing and Bern.

10



5 **Figure S11:** The ROS<sub>OA</sub> and ROS<sub>SOA</sub> vs.  $f_{44}$  color coded by the average OA loading. Symbols represent different emission sources, including ambient aerosols in Beijing and Bern, as well as different emission sources investigated in the laboratory experiments. Error bars represent the standard deviations of the average of all experiments.

## References

- 10 Aiken, A. C., DeCarlo, P. F., Kroll, J. H., Worsnop, D. R., Huffman, J. A., Docherty, K. S., Ulbrich, I. M.,  
 Mohr, C., Kimmel, J. R., Sueper, D., Sun, Y., Zhang, Q., Trimborn, A., Northway, M., Ziemann, P. J.,  
 Canagaratna, M. R., Onasch, T. B., Alfarra, M. R., Prevot, A. S. H., Dommen, J., Duplissy, J., Metzger, A.,  
 Baltensperger, U., and Jimenez, J. L.: O/C and OM/OC Ratios of Primary, Secondary, and Ambient Organic  
 15 Aerosols with High-Resolution Time-of-Flight Aerosol Mass Spectrometry, *Environ. Sci. Technol.*, 42, 4478-  
 4485, 10.1021/es703009q, 2008.

Ng, N. L., Canagaratna, M. R., Jimenez, J. L., Chhabra, P. S., Seinfeld, J. H., and Worsnop, D. R.: Changes in  
 organic aerosol composition with aging inferred from aerosol mass spectra, *Atmos. Chem. Phys.*, 11, 6465-  
 6474, 10.5194/acp-11-6465-2011, 2011.

20